On the modes and loss mechanisms of a high Q mechanical oscillator

Xiao Liu[a]
SFA, Incorporated, Largo, Maryland 20774

S. F. Morse
Naval Research Laboratory, Washington, DC 20375

J. F. Vignola
SFA, Incorporated, Largo, Maryland 20774

D. M. Photiadis, A. Sarkissian, M. H. Marcus, and B. H. Houston
Naval Research Laboratory, Washington, DC 20375

We have performed laser-Doppler vibrometry measurements of the vibration of a double-paddle oscillator. Seven modes with principally out-of-plane motion have been identified. Their resonance frequencies and mode shapes are in excellent agreement with three-dimensional finite element simulations. We have found that the second antisymmetric torsional mode has exceptionally good vibration isolation of its mode shape. This explains its extremely small low temperature internal friction below 10 K (2×10^{-8}). By correlating the internal friction of each mode with features of their mode shapes, a criterion has been established to develop high Q oscillators. © *2001 American Institute of Physics.* [DOI: 10.1063/1.1350599]

High Q double-paddle oscillators (DPOs) based on silicon nanofabrication technology, introduced by Kleiman *et al.*[1] and improved by White and Pohl,[2] have been used in the study of elastic properties of thin film materials.[3,4] Oscillators of similar design have been used in a variety of applications.[5,6] However, extending these designs to microelectromechanical systems (MEMS), a subject of recent interest, has not been as successful. The commonly achieved low Q in MEMS oscillators is a key obstacle limiting the applications of such technology, particularly in the area of rf electronics.[7] In order to improve our understanding of the loss mechanisms that are at work in silicon based oscillators, and in particular to achieve higher Q versions of the DPOs and MEMS oscillators in general, we have investigated the dynamics and loss mechanisms of a DPO.

In this letter we report laser Doppler vibrometry (LDV) measurements of the lowest seven out-of-plane modes of a DPO and the corresponding finite element modeling. Direct LDV measurements have enabled us to establish a detailed finite element method (FEM)[8] predictive capability for the frequencies and mode shapes of the DPO. A detailed prediction of the Q is not possible because of the coupling of the oscillator to its external environment. Nevertheless, an empirical relationship between the mode shapes and internal friction is found which provides insight into the damping mechanisms and may be a useful guide to the development of high Q oscillators using FEM tools.

The silicon oscillator was made of a 300 μm thick, float-zone refined, double-side polished, $\langle 100 \rangle$ oriented, and N-doped silicon substrate with ~ 2 kΩ cm resistivity. Its long axis was along the $\langle 110 \rangle$ orientation. The oscillator was epoxied to an Invar block inside a vacuum chamber (1 mTorr). The oscillator was driven capacitively by an elec-

trode mounted under one of the wings. A second identical electrode under the opposite wing was used as a detector to provide a continuous feedback signal for the drive electronics. This setup enabled stable operation of the oscillator at resonance. Capacitive coupling was achieved by depositing a 400 Å gold film onto the side of the DPO which faced the electrodes. The head and neck were not coated in order to minimize the energy loss caused by metal films[9] to the second antisymmetric torsion mode. For details of the oscillator setup, see Ref. 10.

With the oscillator driven in a selected resonance its out-of-plane surface velocity was measured with a LDV ($\lambda = 780$ nm, 7 mW).[11] Optical access for the laser was made through an optical window in the chamber. The sensitivity of the instrument for reflection from the polished bare silicon surface corresponds to a detection threshold of 0.1–1 Å over the frequency range studied, with relatively little signal averaging. The focused laser spot size on the oscillator was measured by the knife edge technique to be 0.45 mm. A computer-controlled two-axis translation stage was used to position and scan the LDV with respect to the fixed oscillator. The setup is shown in Fig. 1. A surface velocity profile was accumulated through a move-and-measure sequence which was repeated over the entire oscillator area. The move steps ranged between 0.1 and 0.5 mm. At each location the surface velocity was recorded with a 12 bit digitizer at a sampling frequency of 20 kHz and averaged 10–50 times. The measurement was made phase sensitive by the generation of a synchronous trigger from the feedback signal. The resulting velocity profile is shown in Figs. 2(a)–2(c) for three modes. The value plotted is the appropriate Fourier coefficient of the velocity resulting from a fast Fourier transform (FFT) of the measured wave form. The phase is set to maximize the contrast in velocity values.

To compare with the experimental results, the low fre-

Report Documentation Page

Public reporting burden for the collection of information is estimated to average 1 hour per response, including the time for reviewing instructions, searching existing data sources, gathering and maintaining the data needed, and completing and reviewing the collection of information. Send comments regarding this burden estimate or any other aspect of this collection of information, including suggestions for reducing this burden, to Washington Headquarters Services, Directorate for Information Operations and Reports, 1215 Jefferson Davis Highway, Suite 1204, Arlington VA 22202-4302. Respondents should be aware that notwithstanding any other provision of law, no person shall be subject to a penalty for failing to comply with a collection of information if it does not display a currently valid OMB control number.

1. REPORT DATE **2000**	2. REPORT TYPE	3. DATES COVERED **00-00-2000 to 00-00-2000**

4. TITLE AND SUBTITLE **On the modes and loss mechanisms of a high Q mechanical oscillator**	5a. CONTRACT NUMBER
	5b. GRANT NUMBER
	5c. PROGRAM ELEMENT NUMBER
6. AUTHOR(S)	5d. PROJECT NUMBER
	5e. TASK NUMBER
	5f. WORK UNIT NUMBER

7. PERFORMING ORGANIZATION NAME(S) AND ADDRESS(ES) **Naval Research Laboratory,4555 Overlook Avenue SW,Washington,DC,20375**	8. PERFORMING ORGANIZATION REPORT NUMBER

9. SPONSORING/MONITORING AGENCY NAME(S) AND ADDRESS(ES)	10. SPONSOR/MONITOR'S ACRONYM(S)
	11. SPONSOR/MONITOR'S REPORT NUMBER(S)

12. DISTRIBUTION/AVAILABILITY STATEMENT
Approved for public release; distribution unlimited

13. SUPPLEMENTARY NOTES
The original document contains color images.

14. ABSTRACT

15. SUBJECT TERMS

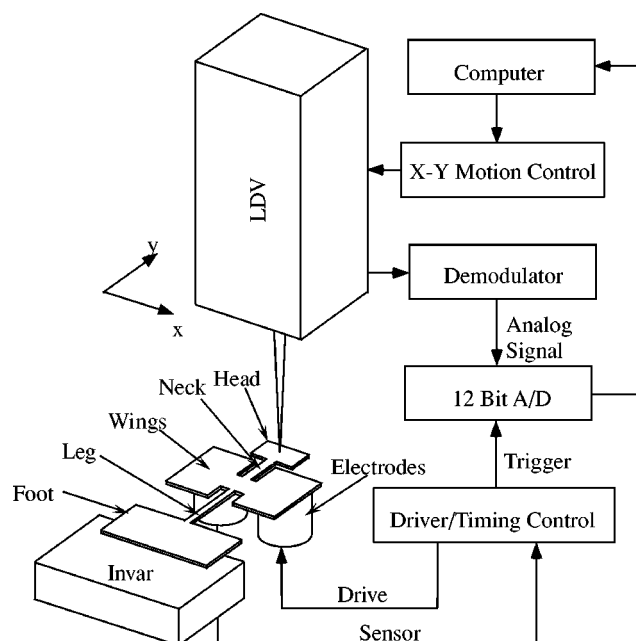| 16. SECURITY CLASSIFICATION OF:			17. LIMITATION OF ABSTRACT	18. NUMBER OF PAGES	19a. NAME OF RESPONSIBLE PERSON
a. REPORT **unclassified**	b. ABSTRACT **unclassified**	c. THIS PAGE **unclassified**		**3**	

FIG. 1. Experimental setup for the LDV measurement of a DPO. The DPO is excited in resonance through capacitive drive and detection under each wing by feedback electronics. The out-of-plane motion of the oscillator surface is measured by the LDV.
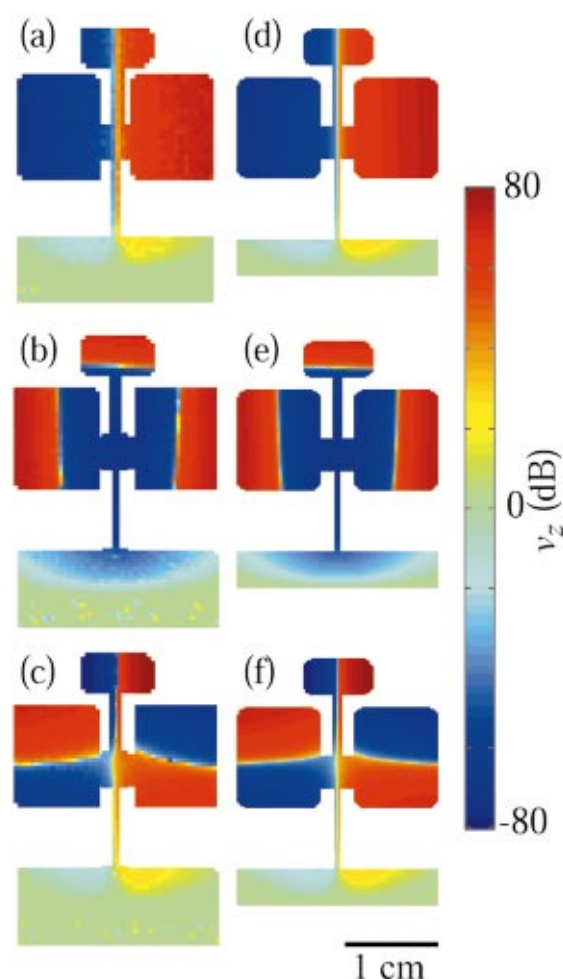

FIG. 2. (Color) Normal component of the surface velocity for three modes of the DPO measured by the LDV (a)–(c) and calculated by the FEM (d)–(f). The modes are the symmetric torsion, flapping, and the second antisymmetric torsion, from top to bottom, respectively. Each is scaled to a common total kinetic energy. The second antisymmetric torsion mode is characterized by the least overall out-of-plane motion of the foot structure. However, since the symmetric torsion mode and the second antisymmetric torsion mode differ only 6 dB in the out-of-plane motion in the foot (see Fig. 3), they are almost indistinguishable in the color scale from −80 to 80 dB given here.

quency eigenfrequencies and mode shapes were computed numerically by using the FEM computer code SARA-3D.[12] A total of 634 three-dimensional (3D) brick elements were used, containing 5041 nodes, with one element along the thickness. The discretization was varied to check for convergence. Rigid boundary conditions were applied to the lower half of the foot where the actual oscillator was epoxied to the Invar base; see Fig. 1. The material parameters of the model were taken to be the room temperature elastic constants of silicon:[13] $c_{11}=165.8$ GPa, $c_{12}=63.94$ GPa, $c_{44}=79.62$ GPa and its mass density: $\rho=2.332$ g/cm^3.

Table I compares the observed room temperature resonance frequencies with the computed eigenfrequencies. We use the same name convention as that introduced in Ref. 10. This level of agreement was achieved only when the oscillator was modeled in significant detail; the geometry was measured directly using a microscope and various aspects such as the beveled edges and rounded corners resulting from the anisotropic wet chemical etch fabrication process[10] were taken into account. Using the low temperature elastic constants, we have also obtained FEM predictions of the frequency shifts, in good agreement with experiment at $T=0.4$ K.

The modal behavior predicted by the finite element model is shown in Figs. 2(d)–2(f) together with the results of the LDV scans. The velocities have been normalized and the color scale is set with respect to the peak velocity. Differences in the oscillator outlines between the measurements and simulations are a result of the finite spot size of the laser and the particular scan pattern used. In addition, the measured scan area includes the foot area which is epoxied to the base; this area is not present in the simulations. In comparison with the LDV scans, the FEM gives an adequate description of the mode shapes and relative amplitudes, even in the unepoxied part of the foot. The success of the FEM model in predicting both mode shapes and resonance frequencies demonstrates that the FEM model captures the relevant physics of the DPO.

The unique feature of the DPO is its extremely small internal friction at low temperature below 10 K, for the second antisymmetric torsion mode. The reason for this is not yet completely understood, nor have its dynamics, such as the strain or stress distribution, been studied. Recent

TABLE I. Comparison of the resonance frequencies f_0 with the eigenfrequencies f_e obtained from the FEM for the seven modes studied.

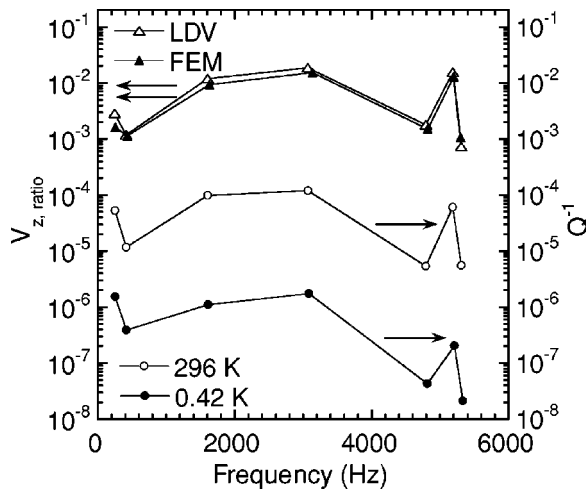| Mode definition	f_0 (Hz)	f_e (Hz)	$\Delta f/f_0$ (%)
1st cantilever	249.88	253.01	1.25
Symmetric torsion	414.77	430.10	3.70
2nd cantilever	1602.7	1629.9	1.70
3rd cantilever	3070.0	3133.7	2.07
1st antisymmetric torsion	4791.6	4817.5	0.54
1st flapping	5185.0	5201.3	0.99
2nd antisymmetric torsion	5307.6	5298.3	−0.18

FIG. 3. Comparison of the measured (LDV) and calculated (FEM) nondimensional root integrated velocity ratio, $V_{z,\text{ratio}}$, for all observed modes with measured internal friction. The LDV data and FEM calculations are plotted with respect to the left axis while the internal friction is referenced to the right axis.

investigations[10] suggest the principal loss mechanism is associated with the epoxy boundary between the silicon and Invar base. LDV scans reveal higher levels of normal velocity on the foot for modes with larger internal friction, in accord with this notion. The strong mode dependence of the internal friction, shown in Fig. 3, together with the fact that this dependence is quite similar at low temperature and room temperature, provides further support for the dominance of attachment losses as the source of damping of the DPO since attachment losses are sensitive to the sample mounting and details of its mechanical coupling to the environment. Inevitably, there are always issues of reproducibility associated with measurements, in which attachment losses are dominant; see Ref. 10 for details. Also shown in Fig. 3 is the square root of the kinetic energy in the foot relative to the total kinetic energy (the in-plane components are negligible),

$$V_{z,\text{ratio}} = \sqrt{\frac{E_{\text{foot}}}{E_{\text{tot}}}} = \sqrt{\frac{\int_{\text{foot}} |v_z|^2 dA}{\int_{\text{osc}} |v_z|^2 dA}}, \tag{1}$$

evaluated using LDV and FEM results. The agreement between the LDV and FEM is not surprising due to the excellent agreement of mode frequencies and mode shapes in Table I and Fig. 2, but the correlation between $V_{z,\text{ratio}}$ and Q^{-1} is striking. This result suggests a relatively simple loss mechanism, which is proportional to the translational motion of the unepoxied part of the foot.

One might hope to develop a simple model explaining the empirical relationship between $V_{z,\text{ratio}}$ and Q^{-1} if the attachment losses are indeed viscoelastic within the glue, or at least are the dominant source of damping. However, mea-

surements of the internal friction of the DPO mounted using a dry clamping method are nearly the same as those mounted with epoxy, and thus viscoelastic dissipation in the glue layer is not relevant. The dissipation due to attachment losses is thus dependent on knowledge of the input impedance of the support structure and may have a nontrivial frequency dependence, although a simple assumption regarding energy transmission to the environment might suffice. On the other hand, for the high Q modes, internal losses may play a role. Indeed, we have found that the temperature dependence of the high Q antisymmetric mode for $T > 10$ K is well accounted for by thermo-elastic dissipation.[14,15] More experimental data, or perhaps a direct measurement of the energy flow through the foot, an aspect requiring a signal to noise ratio beyond our current capability, seems to be needed to fully understand our results.

In conclusion, we have performed LDV measurements of the first seven out-of-plane modes of the DPO and established detailed FEM simulation capability. The simulations correctly predict both the mode shapes and the resonance frequencies of the DPO. We have uncovered an empirical relationship between the mode shapes and the measured Q of the DPO. This relationship enables us to use the FEM modeling capability to improve the Q of the DPO and provides a starting point for the design of high Q MEMS oscillators.

[1] R. N. Kleiman, G. K. Kaminsky, J. D. Reppy, R. Pindak, and D. J. Bishop, Rev. Sci. Instrum. **56**, 2088 (1985).
[2] B. E. White, Jr. and R. O. Pohl, Mater. Res. Soc. Symp. Proc. **356**, 567 (1995).
[3] B. E. White, Jr. and R. O. Pohl, Phys. Rev. Lett. **75**, 4437 (1995).
[4] X. Liu, B. E. White, Jr., R. O. Pohl, E. Iwanizcko, K. M. Jones, A. H. Mahan, B. N. Nelson, R. S. Crandall, and S. Věprek, Phys. Rev. Lett. **78**, 4418 (1997).
[5] R. D. Biggar and J. M. Parpia, Phys. Rev. B **56**, 13638 (1997).
[6] J. Morillo, Q. Su, B. Panchapakesan, M. Wuttig, and D. Novotny, Rev. Sci. Instrum. **69**, 3908 (1998).
[7] C. Ngyen, *Proceedings of the IEEE International Symposium on Circuits and Systems* (IEEE, Hong Kong, 1997).
[8] O. C. Zienkiewizc, *The Finite Element Method* (McGraw–Hill, New York, 1994).
[9] X. Liu, E. J. Thompson, B. E. White, Jr., and R. O. Pohl, Phys. Rev. B **59**, 11767 (1999).
[10] C. L. Spiel and R. O. Pohl, Rev. Sci. Instrum. **72**, 1482 (2001).
[11] Model 1930 LDV, TSI Inc., St. Paul, MN.
[12] H. Allik, R. Dees, S. Moore, and D. Pan, *SARA-3D User's Manual, version 94-2* (BBN Systems and Technologies, New London, CT, 1994).
[13] G. Simmons and H. Wang, *Single Crystal Elastic Constants and Calculated Aggregate Properties: A Handbook* (MIT Press, Cambridge, MA, 1971).
[14] V. B. Braginsky, V. P. Mitranov, and V. I. Panov, *Systems with Small Dissipation* (University of Chicago Press, Chicago, 1985).
[15] J. Kovalik and P. R. Saulson, Rev. Sci. Instrum. **64**, 2942 (1993).